Photosensitized membrane permeabilization requires contact-dependent reactions between photosensitizer and lipids

Isabel O. L. Bacellar,[†,‡] Maria Cecilia Oliveira,[§] Lucas S. Dantas,[†] Elierge B. Costa,[§] Helena C. Junqueira,[†] Waleska K. Martins,[‖] Andrés M. Durantini,[‡] Gonzalo Cosa,[‡] Paolo Di Mascio,[†] Mark Wainwright,[⊥] Ronei Miotto,[§] Rodrigo M. Cordeiro,[§] Sayuri Miyamoto,[†] Mauricio S. Baptista[†,*]

[†]Departamento de Bioquímica, Instituto de Química, Universidade de São Paulo, Av. Prof. Lineu Prestes 748, São Paulo, SP, Brazil, 05508-000.

[‡]Department of Chemistry and Center for Self-Assembled Chemical Structures CSACS/CRMAA, McGill University, 801 Sherbrook Street West, Montreal, QC, Canada, H3A 0B8.

[§]Centro de Ciências Naturais e Humanas, Universidade Federal do ABC, Avenida dos Estados 5001, Santo André, SP, Brazil, 09210-580.

[‖]Universidade Anhanguera de São Paulo, Av. Raimundo Pereira de Magalhães, 3305, São Paulo, SP, Brazil, 05145-200.

⊥School of Pharmacy & Biomolecular Sciences, Liverpool Jonh Moores University, Liverpool, United Kingdom, L3 3AF.

ABSTRACT: Although the general mechanisms of lipid oxidation are known, the chemical steps through which photosensitizers and light permeabilize lipid membranes are still poorly understood. Herein we characterized the products of lipid photooxidation, and their effects on lipid bilayers, also giving insight into their formation pathways. Our experimental system was designed to allow two phenothiazinium-based photosensitizers (methylene blue, MB, and DO15) to deliver the same amount of singlet oxygen molecules per second to 1-palmitoyl-2-oleoyl-*sn*-glycero-3-phosphocholine (POPC) liposome membranes, but to substantially differ in terms of the extent of direct physical contact with lipid double bonds, *i.e.*, DO15 has a 27-times higher co-localization with ω-9 lipid double bonds than MB. Under this condition, DO15 permeabilizes membranes at least one order of magnitude more efficiently than MB, a result which was also valid for liposomes made of polyunsaturated lipids. Quantification of reaction products uncovered a mixture of phospholipid hydroperoxides, alcohols, ketones and aldehydes. Although both photosensitizers allowed the formation of hydroperoxides, the oxidized products that require direct reactions between photosensitizers and lipids are more prevalent in liposomes oxidized by DO15. Membrane permeabilization was always connected with the presence of lipid aldehydes, which cause a substantial decrease in the Gibbs free energy barrier for water permeation. Processes depending on direct contact between photosensitizers and lipids were revealed to be essential for the progress of peroxidation and consequently for aldehyde formation, providing a molecular-level explanation of why membrane binding is so well correlated with the cell-killing efficiency of photosensitizers.

INTRODUCTION

Photosensitized oxidations, which are reactions elicited by the interaction of light with a photosensitizer molecule (PS) in the presence of oxygen, have well-known detrimental biological effects (*e.g.* skin aging and cancer[1] and inhibition of photosynthesis[2–4]). Remarkably, medical technologies have also been ingeniously developed for exploiting these reactions to trigger oxidation of biomolecules and consequently to eliminate cancer cells or pathogens[5,6]. Nevertheless, although the general mechanisms of photosensitized oxidations are known[7], the detailed molecular steps leading to biological injury remain largely uncharacterized[8].

Lipid membranes are important targets of photosensitized oxidations[9–14], undergoing several transformations upon lipid photooxidation. Many of these transformations are accounted to lipid hydroperoxides, which have been detected in photooxidized membranes by various techniques (*e.g.*, mass spectrometry, MS)[15–20]. These oxidized lipids, formed as the primary product of the reaction of singlet oxygen ($^1O_2$) with unsaturated lipids (*i.e.* ene reaction[21]), adopt modified fatty-acyl chain conformations in lipid membranes and lead to lipid lateral phase separation, increase in surface area and decrease in membrane thickness and elastic moduli[10,22]. Yet, the most impacting transformations inflicted on lipids membranes, *i.e.*, those breaking down transmembrane chemical gradients[9,23] (Scheme 1A), remain poorly understood. Although a general scheme of lipid photosensitized oxidation reactions was proposed long ago by Girotti[21] and despite a multitude of studies characterizing biophysical aspects of this phenomenon (*e.g.*, permeabilization rates and transmembrane pore opening)[24–27], there is currently a lack of experimental evidence on the nature of products and elementary steps leading to membrane permeabilization. Underpinning this mechanism is key toward minimizing detrimental biological effects of photooxidations[1,2] and to improving technologies based on PSs (*e.g.*, photodynamic therapy, PDT)[6,28].

$^1O_2$ is usually considered the prevalent species involved in lipid photosensitized oxidations. Diffusing *ca.* 100 nm in water, $^1O_2$ can react with targets that are close but not necessarily in direct contact with PSs[8]. Not surprisingly, given its

far action range and high reactivity, most of the efforts on PS development for medical applications have thus focused on enhancing $^1O_2$ generation[8]. A number of findings however contest the paradigm that a diffusive species (*i.e.* $^1O_2$) is key to causing membrane permeabilization and rather suggest that contact-dependent reactions with excited states of PSs (*e.g.* those involving hydrogen or e^- transfer with the biological target) may be needed instead (Scheme 1B). Firstly, amphiphilic PSs, which partition and insert themselves in membranes, were proven to be the most efficient in experimental models ranging from membrane mimetic systems to cancer cells and multicellular organisms[9,13,29,30]. In fact, when Anderson and Krinsky first reported in the 1970's that liposomes could be lysed by photooxidation, they already questioned whether or not $^1O_2$ was the major player in this phenomenon[31]. Secondly, and contrary to the popular belief that $^1O_2$-derived lipid hydroperoxides permeabilize membranes, there is growing experimental and computational evidence showing that lipid hydroperoxides form stable membranes that sustain chemical gradients[22,32–35]. Thirdly, phospholipid aldehydes bearing truncated fatty-acyl chains have been shown to disrupt chemical gradients when incorporated to membrane mimetic systems and in molecular dynamics simulations[32,34,36–38]. While being a plausible intermediate in membrane permeabilization mechanisms and being a known product of photosensitized oxidations[15], phospholipid aldehydes have as of today yet to be shown to arise *in situ* during photoinduced membrane permeabilization.

Scheme 1. The chemical steps through which photosensitizers (PS) and light permeabilize lipid membranes are still poorly understood (A), with the relative importance of contact-independent pathways and contact dependent pathways remaining to be determined (B).

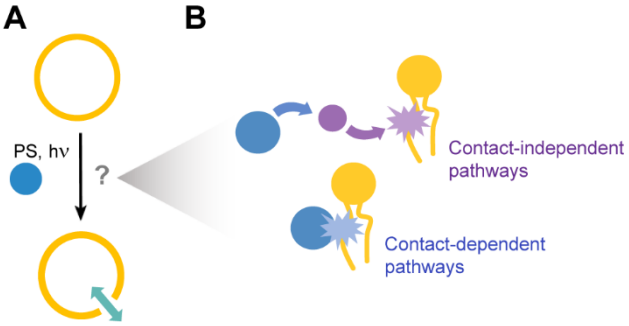

Blue circles represent photosensitizers, while the purple circle represents a mediating, diffusive species. Lipids are represented in gold.

Herein we report experimental and theoretical studies to describing the chemical pathway leading to photoinduced membrane permeabilization. In particular, we designed the experiments in order to quantitatively compare the roles that contact independent and contact-dependent processes have in membrane permeabilization.

RESULTS AND DISCUSSION

Membrane permeabilization and the identity of photooxidized lipids. In order to correlate membrane permeabilization with lipid oxidation and propose mechanistic routes, we compared the photoinduced effects of two phenothiazinium dyes: methylene blue (MB) and DO15 (Figure 1A). The two compounds bear similar photophysical properties ($^1O_2$ generation quantum yield, Φ_Δ = 0.52 and 0.49 ± 0.02, respectively[39]) and are chemically similarly, as they are based on the same chromophore structure, though differing drastically in terms of hydrophobicity (log P = -0.10 and +1.9, respectively[40,41]) and hence of interaction with membranes and membrane damage efficiency[39]. As model membranes, we employed in most of the experiments liposomes made of 1-palmitoyl-2-oleoyl-*sn*-glycero-3-phosphocholine (POPC), which is a lipid bearing a monounsaturated fatty acid (MUFA). Aiming to dissect the impact of lipid oxidation products formed by $^1O_2$ *vs.* by contact-dependent reactions (Scheme 1B), we propose an experimental design in which both PSs delivered almost the same amount of $^1O_2$ to membranes. This was achieved by balancing the experimental conditions (*e.g.*, irradiation wavelength and PS/lipid ratio) with membrane proximity of the photosensitizer and the diffusion range of $^1O_2$ within its excited state lifetime, resulting in MB and DO15 delivering *ca.* 160 and 140 $^1O_2$ molecules s^{-1} to the liposome membrane, respectively (see Supporting Information (SI) for details). Indeed, under this experimental condition, the total $^1O_2$ NIR emission signals coming from MB and DO15 samples endorses that $^1O_2$ is generated in similar quantities for both dyes (Figure S6). It is also noteworthy that in this condition DO15 has a 27-times higher co-localization with ω-9 lipid double bonds than MB, which is due to a 21-fold larger number of photosensitizer molecules partitioning in the membranes (see SI for calculation details) and to a 1.3-fold larger overlap with the distribution of the POPC's ω-9 double bond (Table S2 and Figure S3).

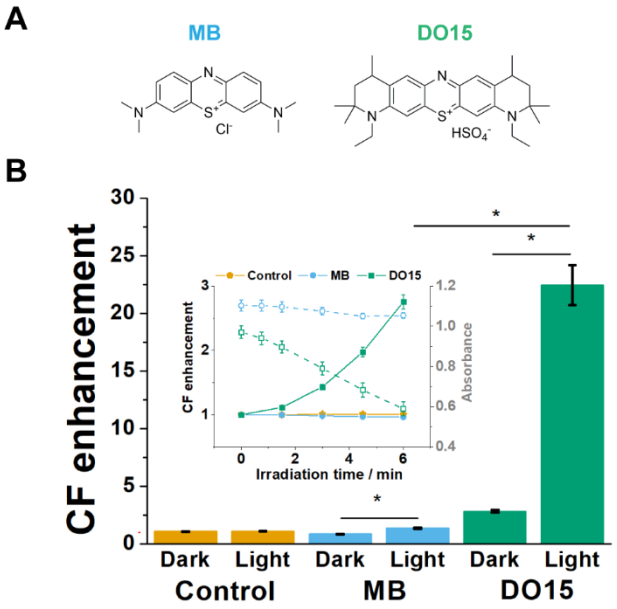

Figure 1. Photosensitized membrane permeabilization by methylene blue (MB) and DO15. (A) Structure of photosensitizers MB and DO15. (B) Fluorescence enhancement of 5(6)-carboxyfluorescein (CF) encapsulated in POPC liposomes (10 mM Tris 0.3 M NaCl, pH = 8) without PS (controls) or with either MB or DO15 (15 μM), after 120 min in the dark or under light exposure (631 nm, 72 ± 1 W m^{-2}). Inset: CF enhancement kinetics (left axis, solid marks) and absorbance variations (right axis,

empty marks – MB: 633 nm; DO15 679 nm) for the first 6 min of irradiation. *denotes p-value < 0.05.

Membrane permeabilization assays (Figure 1B, main graph and inset, left axis), based on the leakage of the probe 5(6)-carboxyfluorescein (CF), show that DO15 permeabilize membranes significantly faster (within minutes) than MB, and that membrane permeabilization is accompanied by a significant decrease in the absorbance of the dye (inset, right axis). Although DO15 is ~16-fold more efficient than MB in terms of the kinetics of membrane permeabilization as a function of irradiation time, after 120 min, both dyes led to liposome permeabilization. It is important to mention that neither DO15 in the absence of light (dark, Figure 1B and Figure S20) nor its bleached species (Figure S7) cause membrane permeabilization. In addition to that, the chelator DTPA did not affect the permeabilization kinetics, ruling out a possible dependence on trace metals (Figure S8). The higher efficiency of DO15 to permeabilize membranes adds to a general trend of membrane permeabilization and PS efficiency being associated to membrane binding, observed for these same PSs in other membrane models[39] and for other classes of PSs in other experimental models[9,13,29,30] This tendency becomes quantitative relevant in our experimental design, in which fluxes of $^1O_2$ molecules reaching the membrane are almost the same, and the level of diffusing triplet excited states reaching the membrane is twice as large for MB than for DO15 (see SI for details). Indeed, permeabilization seems to correlate well with the extent of triplets generated within the membrane that co-localize with lipid double bonds, which is 13 times larger for DO15 than for MB (see SI, section 2.3), suggesting a significant contribution of contact-dependent reactions to the formation of oxidized lipids.

While our photosensitizers and lipid were selected to facilitate mechanistic studies, with the choice for a monounsaturated lipid (POPC) preventing competition from auto-oxidation processes, we understand that it is critical to test whether or not these results also apply for different membrane compositions, including lipid mixtures. Specifically, lipids bearing polyunsaturated fatty acids (PUFAs) are important components of membranes and, by having bis-allylic hydrogens, display a substantially lower energy barrier to fulfill the rate-limiting H-atom abstraction step of peroxidation propagation. To verify if the distinct behavior of DO15 and MB also applies to PUFA phospholipids, we tested how liposomes made of 1-palmitoyl-2-arachidonoyl-*sn*-glycero-3-phosphocholine (PAPC) respond when challenged by MB and DO15 in the same experimental condition as described in Figure 1. Figure S21 shows that the efficiency ratio between MB and DO15 is maintained when oleyl chains are replaced by arachidonoyl, suggesting that the same kind of mechanism operates under both conditions. Even though PAPC favors radical-mediated autooxidation pathways, it also reacts faster than POPC with both triplets and singlet oxygen[21,42–44] (see further discussion below).

HPLC-MS/MS studies of photooxidized liposomes revealed three major oxidation products: lipid hydroperoxides (*m/z* 792.6), alcohols (*m/z* 776.6) and ketones (*m/z* 774.6) (Figure 2A-B, see also Figure 2C for formation kinetics and SI for additional details). While hydroperoxides were the main products for both PSs, DO15 led to more hydroperoxides than MB (45 ± 2 μM and 13 ± 2 μM, respectively, corresponding to 10 ± 1 % and 2.7 ± 0.1 % of the initial POPC concentration), and also to a ~4.5-fold higher concentration of total oxidized lipids (*ca.* 60 μM). Alcohols and ketones, which were formed in smaller quantities than hydroperoxides, totalizing 17 μM and 1 μM for DO15 and MB, respectively (4 % and 0.2 % of the initial POPC concentration), were also quantified directly from the reaction mixture. Both classes of oxidized lipids had been previously described to be products of photosensitized oxidations, but never quantified during the course of membrane permeabilization[16,45]. Our observation that alcohols and ketones occur in equimolar proportions (p-value = 1.000) suggests that they are produced via the Russell mechanism (Scheme 2 – step 4), which is based on the decomposition of a tetroxide intermediate formed upon combination of two peroxyl radicals[46,47].

Since our analysis focuses mainly in the initial steps of membrane photooxidation that are necessary and sufficient for membrane permeabilization, not all classes of oxidized lipid species could be directly detected; indeed the absence of truncated phospholipids bearing oxidized moieties (aldehydes and carboxylic acids[23]) is evident in the analysis described above. In order to enable the detection of these compounds even at low levels, we resorted to their derivatization with the probe 1-pyrenebutyric hydrazide (PBH, see Figure 3A and Figure S12 for adduct structures)[48,49], followed by analysis by HPLC-MS/MS (Figure 3B, see also SI for additional details). Addition of this probe to photooxidized liposomes revealed the formation of phospholipid aldehydes but not of carboxylic acid derivatives. Truncated phospholipid aldehydes with different chain lengths were observed (*m/z* 920.5546, 934.5695 and 946.5700, corresponding to 8-, 9- and 10-carbon chains, respectively) (Figure 3A) and, more importantly, only in those samples that also suffered membrane permeabilization. Liposomes treated with DO15 were permeabilized within minutes upon irradiation, showing a significant increase in the amounts of aldehydes at this timescale (~ 2 μM, Figure 3C). In turn, during the initial steps of irradiation, MB did not permeabilize membranes and did not form aldehydes. Prolonged irradiation (120 min) of MB ultimately led to membrane permeabilization to the same extent as DO15 (*cp.* 3 min, when both samples show CF emission enhancement of ~1.4, see Figure 1B). Remarkably, aldehydes were detected in these samples at concentrations similar to those found in samples irradiated for a 40-fold shorter period with DO15 (Figure 3D, p-value = 0.119), supporting the view that aldehydes are the products that cause membrane permeabilization. These results are the first definitively associating membrane permeabilization with *in situ* aldehyde accumulation.

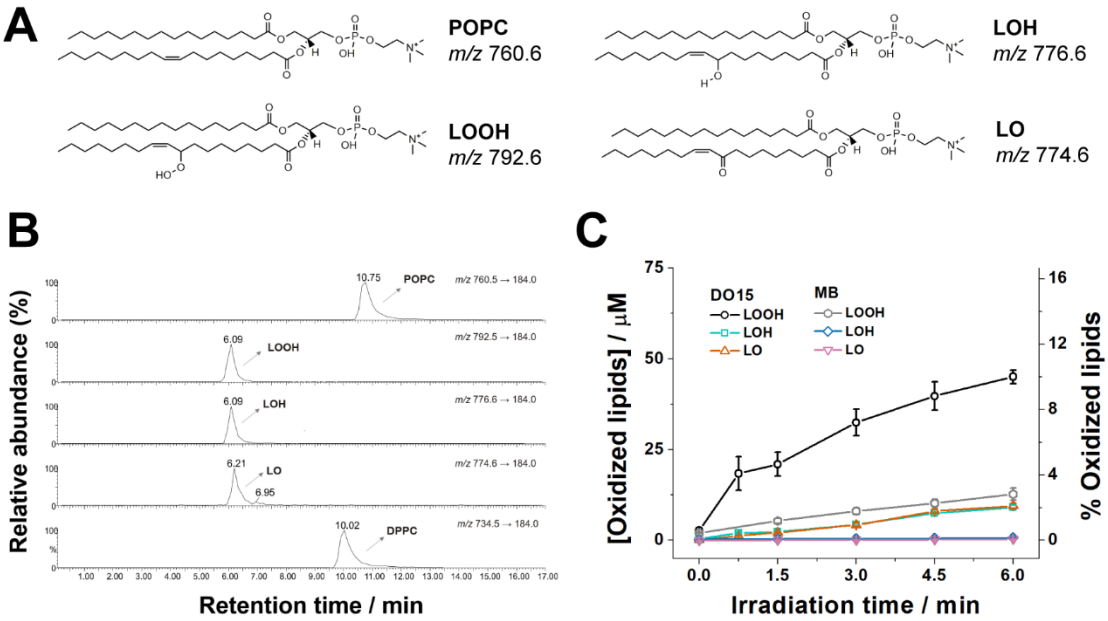

Figure 2. Oxidized lipids detected during photooxidation of POPC liposomes. (A) Structures and detected *m/z* for the $[M+H]^+$ ions for POPC and its major oxidation products: hydroperoxides (LOOH), alcohols (LOH) and ketones (LO), represented here by the 9-Z isomers. (B) Multiple reaction monitoring (MRM) chromatograms for each of the transitions $[M+H]^+ \rightarrow m/z$ 184.0, in ESI+ mode DPPC was employed as internal standard. (C) Concentration of oxidized lipids in μM (left) and in percentage of the initial POPC concentration (right) as a function of irradiation time (631 nm, 72 ± 1 W m^{-2}). [PS] = 15 μM. *denotes p-value < 0.05.

Scheme 1. Chemical pathway to photoinduced membrane permeabilization. The map distinguishes between contact-independent and contact-dependent processes, which rely on $^1O_2$ or on direct reactions between PSs and lipids, respectively.

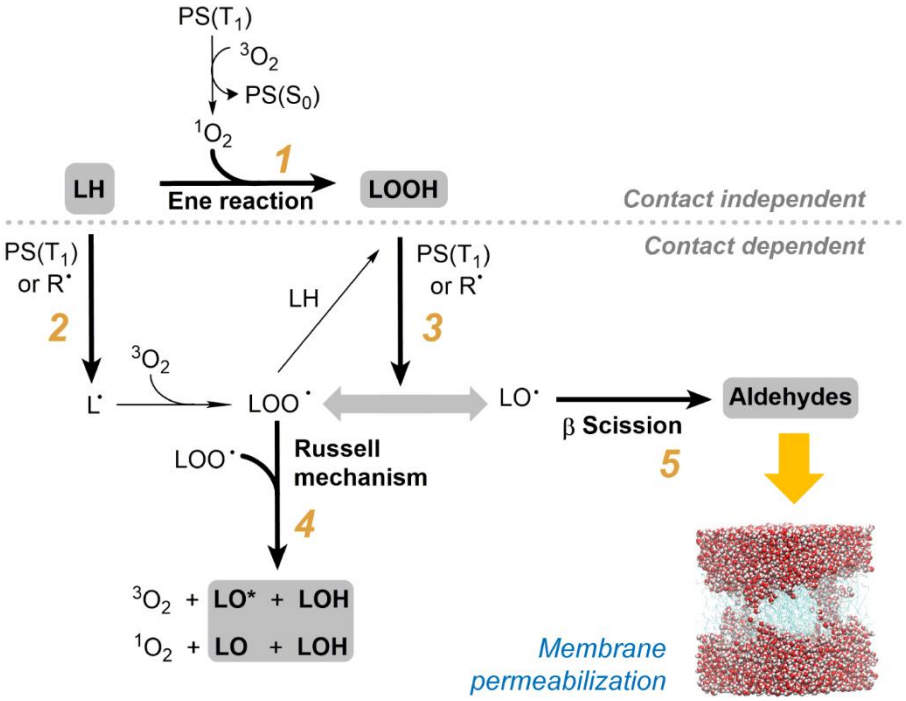

$PS(S_0)$, $PS(T_1)$: PS ground and triplet excited states; $^3O_2$,$^1O_2$: ground and singlet-excited states of oxygen; $R^\bullet$: generic radical species; LH: non-oxidized lipid; $L^\bullet$, $LOO^\bullet$, $LO^\bullet$: lipid carbon-centered, peroxyl and alkoxyl radicals; LOOH, LOH, LO, LO^*: lipid hydroperoxide, alcohol, ketone and excited state ketone. A snapshot of a simulated aldehyde membrane, showing pore opening, is also provided (see SI for details).

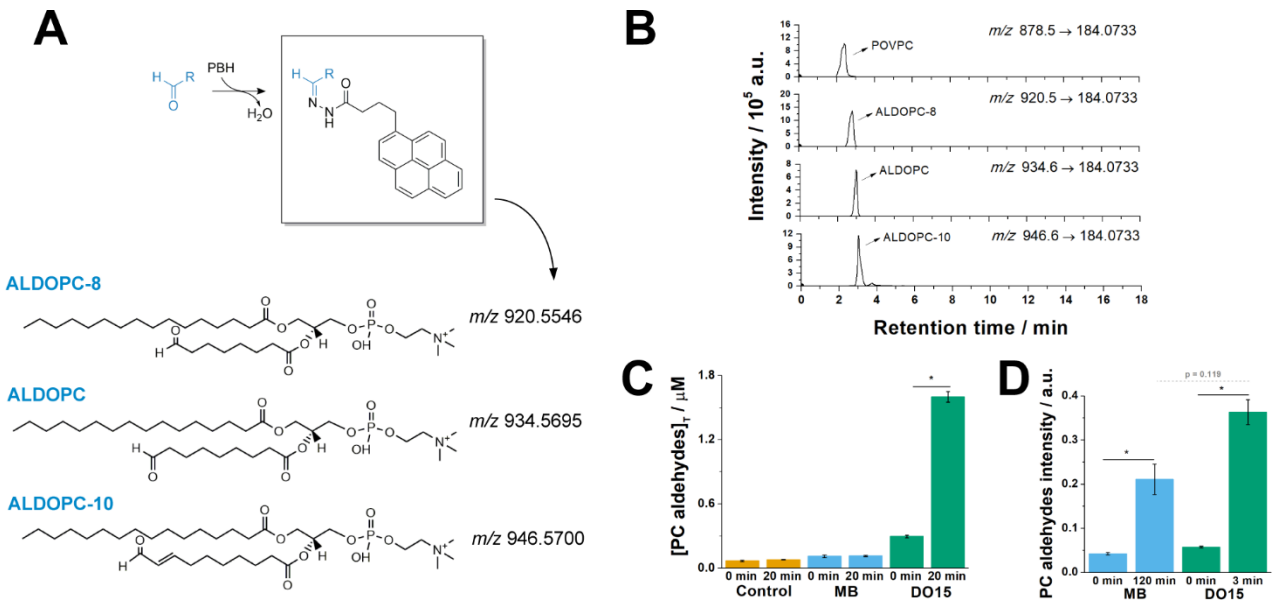

Figure 3. Quantification of POPC-derived aldehydes. (A) Structures of POPC-derived phospholipid aldehydes (ALDOPC-8, ALDOPC and ALDOPC9) and detected m/z for the respective $[M+H]^+$ ions. Aldehydes were detected as PBH adducts, as represented above. (B) Parallel reaction monitoring (PRM) chromatograms for each of the transitions $[M+H]^+ \rightarrow m/z$ 184.0733, in ESI+ mode (POVPC: 1-palmitoyl-2-(5'-oxo-valeroyl)-*sn*-glycero-3-phosphocholine, employed as internal standard). Samples consisted of POPC liposomes irradiated (631 nm, 72 ± 1 W m^{-2}) for 20 min with DO15. (C) Total aldehyde concentration at 0 and 20 min of irradiation without (control) or with PSs. (D) Comparative quantification of total aldehydes at 0 min and at 120 min of irradiation with MB or at 3 min of irradiation with DO15. [PS] = 15 μM. [POPC] was 2.5-fold lower in (C), being the same as for Figure 2, see SI for details. *denotes p-value < 0.05.

The effects of photooxidized lipids. Several factors affect the permeability of solutes through membranes. Excluding the condition associated with the generation of large pores in membranes, they can all be translated into transient changes of the potential energy in the course of solute permeation[50]. Any membrane alteration that causes a decrease in the pathway that solutes need to cross or an increase the diffusion rate of solutes within the membrane will favor permeation. For example, membranes made of shorter chain lipids, are thinner with shallower energy barriers, resulting in higher permeability[51,52]. Obviously, decrease in lipid packing or creation of transient diffusion pathways for solutes will increase permeability[53,54]. But not all physical changes will increase permeability. Interestingly, this seems to be the case of stretching of lipid membranes, with the lack of increase in permeability being explained by the fact that the main barrier to permeation is located in middle of the membrane and is insensitive to stretching[52].

In order to evaluate the biophysical effects of each of the four classes of detected oxidation products, we resorted to molecular dynamics simulations. Table 1 shows the calculated free energy barriers of water permeation through pristine POPC and all the simulated fully oxidized bilayers, thus providing a quantitative comparison of water permeability for the different classes of oxidized lipids. Membranes made of hydroperoxides, alcohols and ketones posed similar permeation barriers as POPC (~30 kJ mol^{-1}). Strikingly, truncated lipid aldehydes, however led to a more than 2-fold decrease in the energy barrier, due to the formation of transmembrane pores (Figure 4E). This result is clearly seen in Figure 4D-E, where aldehyde groups span the whole membrane (D), while water molecules permeate across the bilayer (E). Therefore, our results confirmed the hypothesis that aldehydes cause membrane permeabilization. Also, theorical work performed by others have shown that aldehydes (more than 15%, mol%) cause enough disorganization in the membranes to allow formation of pores[32,55]. Once these pores are formed, membrane stability is lost. Even in the presence of low amounts of aldehydes, simulations predict the formation of transient water pores that somehow increase water permeation[55]. Another important piece of information coming from the simulations is that these transient water pores, which are induced by aldehydes in low concentration, are of single water molecules, *i.e.*, somehow aldehydes simply facilitate water to find new ways across the membranes. The fact that aldehydes increase membrane permeability in low concentrations was also shown by assembling membranes with commercially available aldehydes. For instance, when Ytzhak and Ehrenberg studied the permeabilization effects of ALDOPC and a shorter chain phospholipid aldehyde in egg lecithin liposomes, they observed dissipation of an ionic gradient by employing as little as 2% of any of these aldehyde species, with higher concentrations amplifying this effect[38]. By working with GUVs containing cholesterol saturated and unsaturated lipids, Runas *et al.* observed that increasing the amount of ALDOPC from 0 to 2.5% enhanced in one order of magnitude membrane permeability to a fluorescent, short-chain poly(ethylene glycol) molecule (PEG12-NBD)[36].

Truncated aldehyde phospholipids have two molecular characteristics that make it catalyze a type of shuttle system for water molecules. In the remaining alkyl chain there is enough alkyl groups to work as a membrane anchor, while in the broken chain, which bears the aldehyde group, there is a certain level of hydrogen bonding and flexibility that allows the aldehyde to bind water molecules and to freely move in and out of the membrane surface. In this model, if there are

two aldehydes molecules in different sides of the membranes, there will be a chance for the water to be shuttled from one side to the other of the membrane. This model is endorsed by molecular dynamics simulations[32,55] and is compatible with the experimental data from this work as well as from the literature[36–38], showing that very low concentration of aldehydes is already enough to cause membrane permeabilization (Figure 3D).

Table 1. Gibbs free energy barrier for water permeation from simulated single-component membranes.

	POPC	LOOH	LOH	LO	ALDOPC
ΔG / kJ mol^{-1}	31 ± 3	30 ± 5	30.0 ± 0.3	> 34	12 ± 4

LOOH, LOH, LO, ALDOPC: POPC-derived hydroperoxide, alcohol, ketone and aldehyde, respectively. See SI for calculation details.

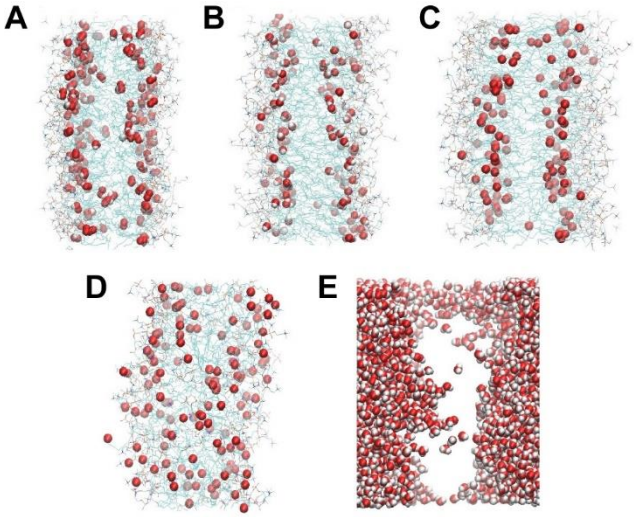

Figure 4. Snapshots from molecular dynamics simulations of oxidized lipid membranes. Single-component membranes were composed by POPC-derived (A) hydroperoxides, (B) alcohols, (C) ketones or (D-E) aldehydes, with the oxidized groups highlighted in red (van der Waals spheres) for A-D. Water molecules were omitted for simplicity, except for (E), in which lipids were omitted instead.

The mechanism of membrane permeation by aldehyde-bearing truncated phospholipids does not seem to apply to other phospholipids bearing shorter alkyl chains. For example, truncated lipids bearing a carboxylic acid contributes to the increase in the disorder of the hydrophobic region of the bilayer, but not enough to lead to pore formation, in a marked contrast to aldehydes.[54] Besides, our experiments did not show the presence of truncated lipids bearing carboxylic acids in the initial steps of photooxidation, in a timeframe that membranes are already leaking in the presence of aldehyde-bearing truncated phospholipids. Another interesting result was obtained by Ytzhak and Ehrenberg, who observed that incorporation of L-α-lysophosphatidylcholine to liposomes did not cause dissipation of ionic gradients in concentrations in which phospholipid aldehydes did[38].

Besides endorsing the permeabilizing effects of aldehydes[22,32–34,55], our simulations confirmed that hydroperoxides form stable membranes in which no pores are observed (Figure 4A, Figure S15A and [35]). Remarkably, alcohols and ketones led to the same result as for hydroperoxides, even though bilayers displayed different membrane thickness, area occupied per lipid and spatial distribution of oxygenated groups (Figure 4B-C, Figure S15B-C and Table S4). The main consequences of forming lipid hydroperoxides is that membranes tend to expand, due to a significant increase in the area per lipid as well as a significant decrease in the stretching modulus[22]. However, membranes made of hydroperoxides are stable and sustain chemical (*e.g.*, sugar) gradients[22]. Interestingly, Gauthier and Joos showed that the overall water membrane permeability remains nearly constant within relevant ranges of area per lipids. The data presented in this manuscript is also in agreement with this effect. We do not rule out that phospholipid hydroperoxides, alcohols and ketones may still contribute to membrane permeabilization via specific interactions between different oxidation products. However, the existence of such a synergistic effect, as well as the role of lipid lateral organization, remains to be investigated.

While hydroperoxides, alcohols and ketones were formed in larger concentration than aldehydes (1.6 ± 0.2 μM after 6 min of irradiation with DO15, *i.e.* ~6-fold smaller than that of alcohols or ketones), only the latter significantly favored water permeation and led to pore opening. Through quantification of multiple lipid oxidation products in different stages of the membrane permeabilization process, we demonstrated that membrane permeabilization correlates with phospholipid aldehyde detection: this is especially evident when we compare samples irradiated with MB for shorter times, when no permeabilization is seen and no aldehydes are detected, *versus* samples irradiated for longer times, when both permeabilization and aldehyde levels are significant. DO15 shows much faster permeabilization kinetics and, indeed, aldehydes can be detected much earlier than for MB. We are thus confident that these theoretical and experimental evidences clearly converge to prove the crucial role of aldehydes in photoinduced membrane permeabilization.

Sources of photooxidized lipids. Understanding the pathways (Scheme 2) behind lipid photooxidation is mandatory in order to control membrane permeabilization, which in biological scenario ultimately determines cell faith between programed cell death pathways or accidental cell death[8,9]. Photosensitized oxidations encompass both direct reactions between PSs and substrates (*e.g.*, lipids) and reactions depending on a mediating species, most often $^1O_2$. As previously discussed, the different efficiencies of DO15 and MB while in a condition where both deliver similar amounts of $^1O_2$ to membranes suggests a key role of contact-dependent steps. This is endorsed by the detection of alcohol and ketones, which not only are not expected from $^1O_2$ chemistry alone but were also formed in proportions consistent with peroxyl radicals being their precursor (Scheme 2 – step 4). Further support to the key role of radical-mediated pathways is provided by the detection of phospholipid aldehydes, as further discussed below.

The initiation and progress of radical-mediated lipid oxidation in the absence of metals relies on contact-dependent reactions of the triplet excited state of PSs, which are prone to abstract hydrogens or donate electrons[7]. Possible targets of

triplets are double bonds (H-abstraction) and/or hydroperoxides (electron donation), which can be pre-formed through the ene reaction[56] (Scheme 2 – steps 2, 3). Consistent with the direct involvement of the PS in these processes, Figure 1B (inset, right axis) shows that membrane permeabilization is invariably coupled to PS bleaching, as characterized by a decrease on the main absorption band of the PSs (630-680 nm). Indeed, spectral changes observed during irradiation confirmed that DO15 extensively bleaches during membrane permeabilization experiments (Figure 5A-C and Figure S16). Not only that, the photobleaching rates of DO15 paralleled the rate of absorption increase at *ca.* 225 nm, which corresponds to the formation of lipids bearing α,β-unsaturated ketones[57] (Figure 5D, see also Figure S9) and proving the fundamental role of contact-dependent reactions for the progress of lipid peroxidation. Compared with a water control, both the photobleaching rate of DO15 (Figure 5B-C) and the consecutive formation of oxidized lipids (Figure 5D) increased in the presence of lipids bearing allylic hydrogens (POPC and 1,2-dioleoyl-*sn*-glycero-3-phosphocholine, DOPC) or hydroperoxides, but not in the presence of saturated lipids (1,2-dipalmitoyl-*sn*-glycero-3-phosphocholine, DPPC). Even though photobleaching rates are very similar in pure POPC and DOPC membranes, experiments carried out in membranes containing a saturated lipid and smaller percentages of POPC or DOPC showed that the photobleaching rates indeed depend on the concentration of double bonds (Figure S17). Yet, in pure unsaturated lipid bilayers the rates converge due to a saturation effect of double bonds concentration. The increase in DO15 photobleaching by unsaturated lipids demonstrates the significance of the abstraction of allylic hydrogens by the PS. These reactions yield lipid carbon-centered radicals, which rapidly react with oxygen and form peroxyl radicals[58], contributing to the buildup of the peroxyl radical pool from which alcohols and ketones emerge. Importantly, the photobleaching rates of MB were shown to be poorly dependent on liposome compositions or even on their presence (Figure 5B), in accordance to the higher hydrophilicity and lower membrane permeabilization efficiency of MB.

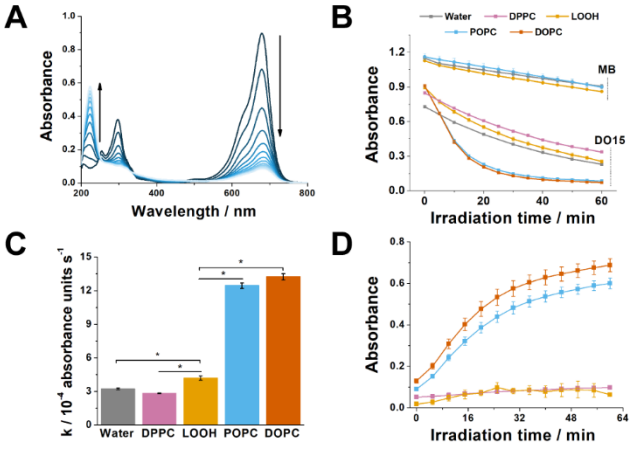

Figure 5. Spectral changes observed upon irradiation of PSs in the presence of liposomes. (A) Absorption spectra of DO15 (15 μM) in the presence of POPC liposomes, at different irradiation times (650 nm, 35 mW, 5 min intervals). (B) Change in the absorbance in the main absorption band of DO15 (graph A, downward arrow) during irradiation in absence or in the presence of DPPC, POPC hydroperoxides (LOOH), POPC and DOPC liposomes. Data is also provided for MB (15 μM) in water, liposomes of POPC and LOOH. (C) Photobleaching rate constants for DO15, obtained from (B). (D) Change in the absorbance in the ketone absorption band (graph A, upward arrow) Of liposomes irradiated in the presence of DO15, in the same conditions as in (B). *denotes p-value < 0.05.

Previous reports showed that hydroperoxides quench the triplet excited state of MB, while also suggesting that this reaction forms alkoxyl radicals[59,60]. The fact that the photolysis of DO15 in the presence of POPC hydroperoxide liposomes indeed showed an increase in dye bleaching rates if compared with photolysis in water (Figure 5C and Figure S16) endorsed the hypothesis that DO15 can also directly produce peroxyl and/or alkoxyl radicals by reacting with hydroperoxides (Scheme 2 – step 3). We highlight that not all -OOH groups of hydroperoxide float on the membrane/water interface and some may localize closer to the original position of lipid unsaturation (Figure 4A); therefore, the distribution of DO15 in the membrane would likely overlap with the distribution of -OOH groups. The hypothesis that DO15 generates oxygenated lipid radicals was confirmed by irradiating liposomes containing DO15 and the fluorogenic probe H_2B-PMHC, which is an α-tocopherol analogue whose fluorescence is enhanced upon reaction with peroxyl or alkoxyl radicals[61] (Figure S18). Not only significant enhancement of H_2B-PMHC's fluorescence occurred in the presence of oxygen (Figure 6A), but also enhancement rates were higher in water than in deuterium oxide (Figure 6B). While we hypothesize that the reasons behind the smaller rates in deuterium oxide might be related to isotopic effects slowing down contact-dependent reactions, we highlight that these results follow the opposite order to what expected for any $^1O_2$-dependent process and endorse that oxygenated lipid radicals generated through contact-dependent reactions are involved in lipid membrane photooxidation.

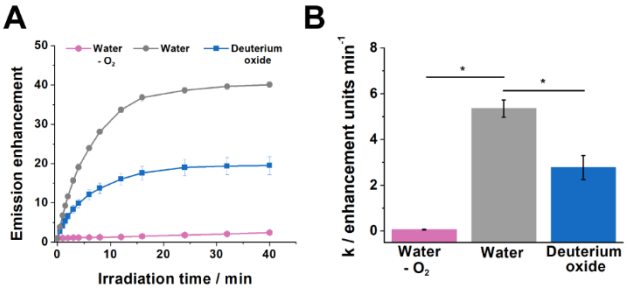

Figure 6. Detection of lipid oxygenated radicals by the fluorogenic probe H_2B-PMHC. (A) Activation kinetics and (B) activation rate constants for H_2B-PMHC in POPC liposomes. Samples were irradiated (634 nm, 1.85 mW cm^{-2}) with DO15 (0.24 μM) in water (argon purged or air-equilibrated) or deuterium oxide-based PBS. *denotes p-value < 0.05.

We finally consider the main reaction that leads to formation of lipid aldehydes in our system, which can be produced either through radical-mediated reactions or through hydroperoxide decomposition, *i.e.* presumably directly from $^1O_2$ products and without the need of contact-dependent processes. In the case of monounsaturated lipids, these processes correspond, respectively, to alkoxyl radical β-scission

(Scheme 2 – step 5 and Scheme 3B) and hydroperoxide Hock cleavage (Scheme 3A)[62,63].

Scheme 3. Possible reactions leading to phospholipid aldehydes and membrane permeabilization. (A) Hydroperoxide Hock cleavage and (B) alkoxyl radical β-scission, for related hydroperoxide and alkoxyl radical structures.

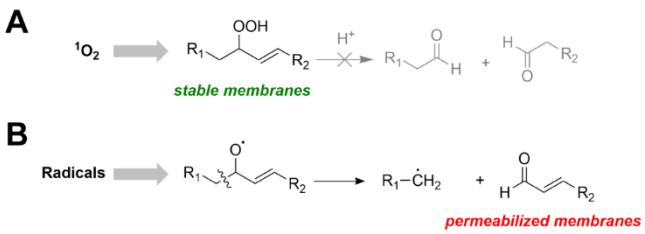

Hock cleavage, though never demonstrated for monounsaturated phospholipids, is commonly proposed as a source of aldehydes directly from other classes of hydroperoxides[23,27,64]. Still, the conditions in which Hock cleavage was shown to occur were invariably either in organic solvents or in thin films of lipids exposed to an undefined atmosphere, usually with an unknown amount of acid added to the sample. Consequently, the role of Hock cleavage in biologically-relevant conditions remains highly controversial. It is also important to mention that the work performed by Morita's group during several decades has never shown any evidence of Hock-cleavage based autooxidation of lipid hydroperoxides[65–68]. Nonetheless and despite the lack of convincing evidences, this mechanism is still frequently mentioned to explain peroxidation progression in membranes as a subsequent step of the hydroperoxide formation. Our data indeed shows that hydroperoxides will rest quietly in lipid membranes, even in conditions that could, in principle, catalyze Hock cleavage, but that actually do not. We observed that giant unilamellar vesicles (GUVs) made of POPC hydroperoxides remained impermeable to sugars independently of pH, similarly to GUVs made of pristine POPC (Figure S19). The fact that membranes kept their impermeability even in pH 3.5 discards the acid catalyzed Hock cleavage as a pathway for phospholipid aldehyde formation under the studied conditions. Not even membranes made of lipids having a polyunsaturated chain, *i.e.*, PAPC and its hydroperoxides, show any relevant permeabilization by lowering down the pH or by adding a Lewis-acid (Fe(III) salt). Note also that this GUV assay is sensitive to measure membrane permeabilization, since PAPC GUVs burst within minutes of exposure to Fe(II), showing that the experimental system responds positively for radical type (Fenton reaction) oxidative damage in the membrane (Figure S19). Moreover, Hock cleavage from POPC hydroperoxides would only yield aldehydes bearing saturated carbon chains, while one of the aldehydes species detected by us has a 10-carbon unsaturated chain (Figure 3A). The formation of this product together with the other two detected species (with 8 and 9-carbon saturated chains) is consistent with alkoxyl radical β-scission (Scheme 2 – step 5, see also SI for details), a pathway relying on radical chemistry and consistent with the production of oxygenated radicals by DO15 and with their role on lipid peroxidation propagation[62,69] Therefore, our experiments provides further evidence that lipid hydroperoxides do not suffer direct breakage by Hock cleavage, supporting the need for direct-contact reactions that lead to the formation of radicals that through alkoxyl radical β-scission ultimately yield truncated aldehydes. These, in turn, start membrane permeabilization, as summarized in Schemes 2 and 3. The permeabilization experiment performed with PAPC liposomes (Figure S21), as well as previously-reported permeabilization experiments carried out in soy-lecithin liposomes (containing 39% of PUFAs)[39] provides evidence that contact-dependent pathways also matter for membranes made of PUFA lipids. Since the timeframe of the photoinduced processes is a lot shorter than that of the autooxidations processes, the contact-dependent reactions, which govern photoinduced permeabilization in membranes bearing only MUFAs also seem to be governing permeabilization of membranes bearing PUFAs. Thus, these results suggest that the findings reported herein and the proposed chemical pathway are valid for different lipid compositions.

The original definition of type I and type II photooxidations by Foote has as a hallmark the contrast between processes depending on direct contact between PSs and substrates or alternatively relying on diffusive, reactive species[7,70]. Hence, our data explains the key role of contact-dependent pathways for improving photodynamic efficiency, and suggests that the efficacy of PSs can be considerably improved by aiming at targets for direct reactions and expanding their action mechanism beyond $^1O_2$ generation[71]. Interestingly, natural PSs such as flavin and pterins also seems to oxidize biological substrates preferentially through contact-dependent reactions[43,72,73]. We envisage several implications of this knowledge. For example, since membrane permeabilization depends on redox reactions, which are likely to cause photosensitizer bleaching, finding ways to replenish photosensitizers may be a yet to be explored route to allow the design of better photosensitizing agents. Likewise, in order to either increase or avoid damages induced by photosensitized oxidations one can respectively try to increase or avoid accumulation of lipid aldehydes. We are confident that our work will stimulate studies in more complex lipid compositions, as well as, studies aiming to better understand cell death pathways that depend on lipid oxidation, such as ferroptosis[74]. Since membrane damage will depend on the molecular contact between the photosensitizer and the lipid, and not so much on diffusive species, one may start to develop efficient photoinduced organelle-depletion methods.

CONCLUSION

The involvement of lipid carbon-centered, alkoxyl and peroxyl radicals in the progression of lipid peroxidation is a well-known fact[21]. However, the specific details of how these species are actually formed during photosensitized oxidations and lead to membrane permeabilization has remained elusive. By comparing two PSs with similar intrinsic photophysical and photochemical properties but differing in terms of membrane permeabilization efficiencies, we showed that membrane permeabilization is associated with aldehyde production, which can only occur when there are direct reactions between the triplet excited state of the PS and the major targets in the lipid membrane, *i.e.* lipid unsaturations and -OOH groups formed after the initial ene reaction with $^1O_2$. These results, as well as the major reactions operating under membrane photooxidation, are summarized in Scheme 2. The role of contact-

dependent processes in biological photooxidations is often considered secondary to $^1O_2$-mediated oxidations, and consequently $^1O_2$ production is usually the main parameter considered for the development of new PSs. However, our results demonstrate that for a PS to fully compromise membrane function requires its sacrifice through contact-dependent reactions. Therefore, activation/suppression of PS replenishment could be explored as an effective tool to maximize or counter the effects of photosensitized oxidations. We are confident that the roadmap presented herein will provide mechanistic guidelines for further developments in photomedicine and photoprotection.

ASSOCIATED CONTENT

Supporting Information. Computational and experimental methods, additional data for membrane permeabilization, binding, oxidized lipid analysis, photobleaching, H_2B-PMHC activation pathway, giant unilamellar vesicle permeability and molecular dynamics simulations. This material is available free of charge via the Internet at http://pubs.acs.org.

AUTHOR INFORMATION

Corresponding Author

*baptista@iq.usp.br

Notes

The authors declare no competing financial interests.

ACKNOWLEDGMENT

Fundação de Amparo à Pesquisa do Estado de São Paulo (FAPESP) is acknowledged for financial support (grants 2012/50680-5 and 2013/07937-8). Authors also acknowledge Núcleo de Apoio à Pesquisa em Tecnologia Fotoquímica (NAP-Phototech) and individual FAPESP fellowships (2013/11640-0 and 2015/22935-7). Fernanda M. Prado is acknowledged for assisting some of the HPLC-MS analyses and prof. Frank H. Quina (IQUSP) for revising the manuscript.

REFERENCES

(1) Sander, C. S.; Hamm, F.; Elsner, P.; Thiele, J. J. Oxidative Stress in Malignant Melanoma and Non-Melanoma Skin Cancer. *Br. J. Dermatol.* **2003**, *148* (5), 913–922.

(2) Aro, E.-M.; Virgin, I.; Andersson, B. Photoinhibition of Photosystem II. Inactivation, Protein Damage and Turnover. *Biochim. Biophys. Acta - Bioenerg.* **1993**, *1143* (2), 113–134.

(3) Anthony, J. R.; Warczak, K. L.; Donohue, T. J. A Transcriptional Response to Singlet Oxygen, a Toxic Byproduct of Photosynthesis. *Proc. Natl. Acad. Sci.* **2005**, *102* (18), 6502–6507.

(4) Triantaphylides, C.; Krischke, M.; Hoeberichts, F. A.; Ksas, B.; Gresser, G.; Havaux, M.; Van Breusegem, F.; Mueller, M. J. Singlet Oxygen Is the Major Reactive Oxygen Species Involved in Photooxidative Damage to Plants. *Plant Physiol.* **2008**, *148* (2), 960–968.

(5) Castano, A. P.; Demidova, T. N.; Hamblin, M. R. Mechanisms in Photodynamic Therapy: Part Two - Cellular Signaling, Cell Metabolism and Modes of Cell Death. *Photodiagnosis Photodyn. Ther.* **2005**, *2* (1), 1–23.

(6) Dolmans, D. E. J. G. J.; Fukumura, D.; Jain, R. K. Photodynamic Therapy for Cancer. *Nat. Rev. Cancer* **2003**, *3*, 380–387.

(7) Baptista, M. S.; Cadet, J.; Di Mascio, P.; Ghogare, A. A.; Greer, A.; Hamblin, M. R.; Lorente, C.; Nunez, S. C.; Ribeiro, M. S.; Thomas, A. H.; Vignoni, M.; Yoshimura, T. M. Type I and Type II Photosensitized Oxidation Reactions: Guidelines and Mechanistic Pathways. *Photochem. Photobiol.* **2017**, *93* (4), 912–919.

(8) Bacellar, I. O. L.; Tsubone, T.; Pavani, C.; Baptista, M. Photodynamic Efficiency: From Molecular Photochemistry to Cell Death. *Int. J. Mol. Sci.* **2015**, *16* (9), 20523–20559.

(9) Tsubone, T. M.; Martins, W. K.; Pavani, C.; Junqueira, H. C.; Itri, R.; Baptista, M. S. Enhanced Efficiency of Cell Death by Lysosome-Specific Photodamage. *Sci. Rep.* **2017**, *7* (1), 6734.

(10) Itri, R.; Junqueira, H. C.; Mertins, O.; Baptista, M. S. Membrane Changes under Oxidative Stress: The Impact of Oxidized Lipids. *Biophys. Rev.* **2014**, *6* (1), 47–61.

(11) Sonoike, K. Various Aspects of Inhibition of Photosynthesis under Light/Chilling Stress: "Photoinhibition at Chilling Temperatures" versus "Chilling Damage in the Light." *J. Plant Res.* **1998**, *111* (1), 121–129.

(12) Labuza, T. P.; Dugan, L. R. Kinetics of Lipid Oxidation in Foods. *C R C Crit. Rev. Food Technol.* **1971**, *2* (3), 355–405.

(13) Xu, S.; Chisholm, A. D. Highly Efficient Optogenetic Cell Ablation in C. Elegans Using Membrane-Targeted MiniSOG. *Sci. Rep.* **2016**, *6* (1), 21271.

(14) Roqueiro, G.; Facorro, G. B.; Huarte, M. G.; Rubín de Celis, E.; García, F.; Maldonado, S.; Maroder, H. Effects of Photooxidation on Membrane Integrity in Salix Nigra Seeds. *Ann. Bot.* **2010**, *105* (6), 1027–1034.

(15) Thomas, A. H.; Catalá, Á.; Vignoni, M. Soybean Phosphatidylcholine Liposomes as Model Membranes to Study Lipid Peroxidation Photoinduced by Pterin. *Biochim. Biophys. Acta - Biomembr.* **2016**, *1858* (1), 139–145.

(16) Melo, T.; Santos, N.; Lopes, D.; Alves, E.; Maciel, E.; Faustino, M. A. F.; Tomé, J. P. C.; Neves, M. G. P. M. S.; Almeida, A.; Domingues, P.; Segundo, M. A.; Domingues, M. R. M. Photosensitized Oxidation of Phosphatidylethanolamines Monitored by Electrospray Tandem Mass Spectrometry. *J. Mass Spectrom.* **2013**, *48* (12), 1357–1365.

(17) Wolnicka-Glubisz, A.; Lukasik, M.; Pawlak, A.; Wielgus, A.; Niziolek-Kierecka, M.; Sarna, T. Peroxidation of Lipids in Liposomal Membranes of Different Composition Photosensitized by Chlorpromazine. *Photochem. Photobiol. Sci.* **2009**, *8* (2), 241–247.

(18) Rodriguez, M. E.; Kim, J.; Delos Santos, G. B.; Azizuddin, K.; Berlin, J.; Anderson, V. E.; Kenney, M. E.; Oleinick, N. L. Binding to and Photo-Oxidation of Cardiolipin by the Phthalocyanine Photosensitizer Pc 4. *J. Biomed. Opt.* **2010**, *15* (5), 051604.

(19) Kim, J.; Minkler, P. E.; Salomon, R. G.; Anderson, V. E.; Hoppel, C. L. Cardiolipin: Characterization of Distinct Oxidized Molecular Species. *J. Lipid Res.* **2011**, *52* (1), 125–135.

(20) Kim, J.; Fujioka, H.; Oleinick, N. L.; Anderson, V. E. Photosensitization of Intact Heart Mitochondria by the Phthalocyanine Pc 4: Correlation of Structural and Functional Deficits with Cytochrome c Release. *Free Radic. Biol. Med.* **2010**, *49* (5), 726–732.

(21) Girotti, A. W. Photosensitized Oxidation of Membrane Lipids: Reaction Pathways, Cytotoxic Effects, and Cytoprotective Mechanisms. *J. Photochem. Photobiol. B Biol.* **2001**, *63* (1–3), 103–113.

(22) Weber, G.; Charitat, T.; Baptista, M. S.; Uchoa, A. F.; Pavani, C.; Junqueira, H. C.; Guo, Y.; Baulin, V. A.; Itri, R.; Marques, C. M.; Schroder, A. P. Lipid Oxidation Induces Structural Changes in Biomimetic Membranes. *Soft Matter* **2014**, *10* (24), 4241–4247.

(23) Caetano, W.; Haddad, P. S.; Itri, R.; Severino, D.; Vieira, V. C.; Baptista, M. S.; Schröder, A. P.; Marques, C. M. Photo-Induced Destruction of Giant Vesicles in Methylene Blue Solutions. *Langmuir* **2007**, *23* (3), 1307–1314.

(24) Mertins, O.; Bacellar, I. O. L.; Thalmann, F.; Marques, C. M.; Baptista, M. S.; Itri, R. Physical Damage on Giant Vesicles Membrane as a Result of Methylene Blue Photoirradiation. *Biophys. J.* **2014**, *106* (1), 162–171.

(25) Heuvingh, J.; Bonneau, S. Asymmetric Oxidation of Giant Vesicles Triggers Curvature-Associated Shape Transition and Permeabilization. *Biophys. J.* **2009**, *97* (11), 2904–2912.

(26) Kerdous, R.; Heuvingh, J.; Bonneau, S. Photo-Dynamic Induction of Oxidative Stress within Cholesterol-Containing Membranes: Shape Transitions and Permeabilization. *Biochim.*

Biophys. Acta **2011**, *1801*, 2965–2972.

(27) Sankhagowit, S.; Wu, S. H.; Biswas, R.; Riche, C. T.; Povinelli, M. L.; Malmstadt, N. The Dynamics of Giant Unilamellar Vesicle Oxidation Probed by Morphological Transitions. *Biochim. Biophys. Acta - Biomembr.* **2014**, *1838* (10), 2615–2624.

(28) Scholz, S.; Kondakov, D.; Lüssem, B.; Leo, K. Degradation Mechanisms and Reactions in Organic Light-Emitting Devices. *Chem. Rev.* **2015**, *115* (16), 8449–8503.

(29) Pavani, C.; Iamamoto, Y.; Baptista, M. S. Mechanism and Efficiency of Cell Death of Type II Photosensitizers: Effect of Zinc Chelation. *Photochem. Photobiol.* **2012**, *88* (4), 774–781.

(30) Ben Amor, T.; Jori, G. Sunlight-Activated Insecticides: Historical Background and Mechanisms of Phototoxic Activity. *Insect Biochem. Mol. Biol.* **2000**, *30* (10), 915–925.

(31) Anderson, S. M.; Krinsky, N. I. Protective Action of Carotenoid Pigments against Photodynamic Damage to Liposomes. *Photochem. Photobiol.* **1973**, *18* (5), 403–408.

(32) Boonnoy, P.; Jarerattanachat, V.; Karttunen, M.; Wong-ekkabut, J. Bilayer Deformation, Pores, and Micellation Induced by Oxidized Lipids. *J. Phys. Chem. Lett.* **2015**, *6* (24), 4884–4888.

(33) Yusupov, M.; Van der Paal, J.; Neyts, E. C.; Bogaerts, A. Synergistic Effect of Electric Field and Lipid Oxidation on the Permeability of Cell Membranes. *Biochim. Biophys. Acta - Gen. Subj.* **2017**, *1861* (4), 839–847.

(34) Van der Paal, J.; Neyts, E. C.; Verlackt, C. C. W.; Bogaerts, A. Effect of Lipid Peroxidation on Membrane Permeability of Cancer and Normal Cells Subjected to Oxidative Stress. *Chem. Sci.* **2016**, *7* (1), 489–498.

(35) Neto, A. J. P.; Cordeiro, R. M. Molecular Simulations of the Effects of Phospholipid and Cholesterol Peroxidation on Lipid Membrane Properties. *Biochim. Biophys. Acta - Biomembr.* **2016**, *1858* (9), 2191–2198.

(36) Runas, K. A.; Malmstadt, N. Low Levels of Lipid Oxidation Radically Increase the Passive Permeability of Lipid Bilayers. *Soft Matter* **2015**, *11* (3), 499–505.

(37) Runas, K. A.; Acharya, S. J.; Schmidt, J. J.; Malmstadt, N. Addition of Cleaved Tail Fragments during Lipid Oxidation Stabilizes Membrane Permeability Behavior. *Langmuir* **2016**, *32* (3), 779–786.

(38) Ytzhak, S.; Ehrenberg, B. The Effect of Photodynamic Action on Leakage of Ions through Liposomal Membranes That Contain Oxidatively Modified Lipids. *Photochem. Photobiol.* **2014**, *90* (4), 796–800.

(39) Bacellar, I. O. L.; Pavani, C.; Sales, E. M.; Itri, R.; Wainwright, M.; Baptista, M. S. Membrane Damage Efficiency of Phenothiazinium Photosensitizers. *Photochem. Photobiol.* **2014**, *90* (4), 801–813.

(40) Wainwright, M.; Giddens, R. M. Phenothiazinium Photosensitisers: Choices in Synthesis and Application. *Dye. Pigment.* **2003**, *57* (3), 245–257.

(41) Noodt, B. B.; Rodal, G. H.; Wainwright, M.; Peng, Q.; Horobin, R.; Nesland, J. M.; Berg, K. Apoptosis Induction by Different Pathways with Methylene Blue Derivative and Light from Mitochondrial Sites in V79 Cells. *Int. J. cancer* **1998**, *75* (6), 941–948.

(42) Tanielian, C.; Mechin, R. Reaction and Quenching of Singlet Molecular Oxygen with Esters of Polyunsaturated Fatty Acids. *Photochem. Photobiol.* **1994**, *59* (3), 263–268.

(43) Huvaere, K.; Cardoso, D. R.; Homem-De-Mello, P.; Westermann, S.; Skibsted, L. H. Light-Induced Oxidation of Unsaturated Lipids as Sensitized by Flavins. *J. Phys. Chem. B* **2010**, *114* (16), 5583–5593.

(44) Chacon, J. N.; McLearie, J.; Sinclair, R. S. Singlet Oxygen Yields and Radical Contributions in the Dye-Sensitised Photo-Oxidation in Methanol of Esters of Polyunsaturated Fatty Acids (Oleic, Linoleic, Linolenic and Arachidonic). *Photochem. Photobiol.* **1988**, *47* (5), 647–656.

(45) Luo, D.; Li, N.; Carter, K. A.; Lin, C.; Geng, J.; Shao, S.; Huang, W.-C.; Qin, Y.; Atilla-Gokcumen, G. E.; Lovell, J. F. Rapid Light-Triggered Drug Release in Liposomes Containing Small Amounts of Unsaturated and Porphyrin-Phospholipids. *Small* **2016**, *12* (22), 3039–3047.

(46) Russell, G. A. Deuterium-Isotope Effects in the Autoxidation of Aralkyl Hydrocarbons. Mechanism of the Interaction of Peroxy Radicals. *J. Am. Chem. Soc.* **1957**, *79* (14), 3871–3877.

(47) Miyamoto, S.; Martinez, G. R.; Medeiros, M. H. G.; Di Mascio, P. Singlet Molecular Oxygen Generated from Lipid Hydroperoxides by the Russell Mechanism: Studies Using 18 O-Labeled Linoleic Acid Hydroperoxide and Monomol Light Emission Measurements. *J. Am. Chem. Soc.* **2003**, *125* (20), 6172–6179.

(48) Mansano, F. V.; Kazaoka, R. M. A.; Ronsein, G. E.; Prado, F. M.; Genaro-Mattos, T. C.; Uemi, M.; Mascio, P. Di; Miyamoto, S. Highly Sensitive Fluorescent Method for the Detection of Cholesterol Aldehydes Formed by Ozone and Singlet Molecular Oxygen. *Anal. Chem.* **2010**, *82* (16), 6775–6781.

(49) Nohta, H.; Sonoda, J.; Yoshida, H.; Satozono, H.; Ishida, J.; Yamaguchi, M. Liquid Chromatographic Determination of Dicarboxylic Acids Based on Intramolecular Excimer-Forming Fluorescence Derivatization. *J. Chromatogr. A* **2003**, *1010* (1), 37–44.

(50) Qiao, B.; Olvera de la Cruz, M. Driving Force for Water Permeation Across Lipid Membranes. *J. Phys. Chem. Lett.* **2013**, *4* (19), 3233–3237.

(51) Sugii, T.; Takagi, S.; Matsumoto, Y. A Molecular-Dynamics Study of Lipid Bilayers: Effects of the Hydrocarbon Chain Length on Permeability. *J. Chem. Phys.* **2005**, *123* (18), 184714.

(52) Gauthier, A.; Joós, B. Stretching Effects on the Permeability of Water Molecules across a Lipid Bilayer. *J. Chem. Phys.* **2007**, *127* (10), 105104.

(53) Shinoda, W. Permeability across Lipid Membranes. *Biochim. Biophys. Acta - Biomembr.* **2016**, *1858* (10), 2254–2265.

(54) Shinoda, W.; Mikami, M.; Baba, T.; Hato, M. Molecular Dynamics Study on the Effects of Chain Branching on the Physical Properties of Lipid Bilayers: 2. Permeability. *J. Phys. Chem. B* **2004**, *108* (26), 9346–9356.

(55) Lis, M.; Wizert, A.; Przybylo, M.; Langner, M.; Swiatek, J.; Jungwirth, P.; Cwiklik, L. The Effect of Lipid Oxidation on the Water Permeability of Phospholipids Bilayers. *Phys. Chem. Chem. Phys.* **2011**, *13* (39), 17555.

(56) Bachowski, G. J.; Ben-Hur, E.; Girotti, A. W. Phthalocyanine-Sensitized Lipid Peroxidation in Cell Membranes: Use of Cholesterol and Azide as Probes of Primary Photochemistry. *J. Photochem. Photobiol. B.* **1991**, *9* (3–4), 307–321.

(57) Woodward, R. B. Structure and the Absorption Spectra of α,β-Unsaturated Ketones. *J. Am. Chem. Soc.* **1941**, *63* (4), 1123–1126.

(58) Yin, H.; Xu, L.; Porter, N. A. Free Radical Lipid Peroxidation: Mechanisms and Analysis. *Chem. Rev.* **2011**, *111* (10), 5944–5972.

(59) Tanielian, C.; Mechin, R.; Shakirullah, M. Origin of Dye Bleaching and Polymer Degradation in the Methylene Blue-Sensitized Photo-Oxygenation of Polybutadiene. *J. Photochem. Photobiol. A Chem.* **1992**, *64* (2), 191–199.

(60) Tanielian, C.; Mechin, R. Alkyl Hydroperoxides as Electron Donors in Photochemical Reactions. *J. Photochem. Photobiol. A Chem.* **1997**, *107* (1–3), 291–293.

(61) Krumova, K.; Friedland, S.; Cosa, G. How Lipid Unsaturation, Peroxyl Radical Partitioning, and Chromanol Lipophilic Tail Affect the Antioxidant Activity of α-Tocopherol: Direct Visualization via High-Throughput Fluorescence Studies Conducted with Fluorogenic α-Tocopherol Analogues. *J. Am. Chem. Soc.* **2012**, *134* (24), 10102–10113.

(62) Gardner, H. W. Oxygen Radical Chemistry of Polyunsaturated Fatty Acids. *Free Radic. Biol. Med.* **1989**, *7* (1), 65–86.

(63) Hock Rearrangement. In *Comprehensive Organic Name Reactions and Reagents*; John Wiley & Sons, Inc.: Hoboken, NJ, USA, 2010.

(64) Schneider, C.; Porter, N. A.; Brash, A. R. Routes to 4-Hydroxynonenal: Fundamental Issues in the Mechanisms of Lipid Peroxidation. *J. Biol. Chem.* **2008**, *283* (23), 15539–15543.

(65) Morita, M.; Fujimaki, M. Non-Hydroperoxy-Type Peroxides as Autocatalysts of Lipid Autoxidation. *Agric. Biol. Chem.* **1973**, *37* (5), 1213–1214.

(66) Morita, M.; Tokita, M. Courses of Aldehyde Formation during Linoleate Autoxidation and Some Information about Precursors and Mechanism. *Chem. Phys. Lipids* **1993**, *66* (1–2), 13–22.

(67) Morita, M.; Tokita, M. Evaluation of the Role of

Hydroperoxides in the Formation of Aldehydes during Linoleate Autoxidation. *Chem. Phys. Lipids* **1990**, *56* (2–3), 209–215.

(68) Morita, M.; Tokita, M. The Real Radical Generator Other than Main-Product Hydroperoxide in Lipid Autoxidation. *Lipids* **2006**, *41* (1), 91–95.

(69) Paul, H.; Small, R. D.; Scaiano, J. C. Hydrogen Abstraction by Tert-Butoxy Radicals. A Laser Photolysis and Electron Spin Resonance Study. *J. Am. Chem. Soc.* **1978**, *100* (14), 4520–4527.

(70) Foote, C. S. Mechanisms of Photosensitized Oxidation. *Science* **1968**, *162* (3857), 963–970.

(71) Albani, B. A.; Peña, B.; Leed, N. A.; de Paula, N. A. B. G.; Pavani, C.; Baptista, M. S.; Dunbar, K. R.; Turro, C. Marked Improvement in Photoinduced Cell Death by a New Tris-Heteroleptic Complex with Dual Action: Singlet Oxygen Sensitization and Ligand Dissociation. *J. Am. Chem. Soc.* **2014**, *136* (49), 17095–17101.

(72) Petroselli, G.; Dántola, M. L.; Cabrerizo, F. M.; Capparelli, A. L.; Lorente, C.; Oliveros, E.; Thomas, A. H. Oxidation of 2′-Deoxyguanosine 5′-Monophosphate Photoinduced by Pterin: Type I versus Type II Mechanism. *J. Am. Chem. Soc.* **2008**, *130* (10), 3001–3011.

(73) Cardoso, D. R.; Olsen, K.; Skibsted, L. H. Mechanism of Deactivation of Triplet-Excited Riboflavin by Ascorbate, Carotenoids, and Tocopherols in Homogeneous and Heterogeneous Aqueous Food Model Systems. *J. Agric. Food Chem.* **2007**, *55* (15), 6285–6291.

(74) Stockwell, B. R.; Friedmann Angeli, J. P.; Bayir, H.; Bush, A. I.; Conrad, M.; Dixon, S. J.; Fulda, S.; Gascón, S.; Hatzios, S. K.; Kagan, V. E.; Noel, K.; Jiang, X.; Linkermann, A.; Murphy, M. E.; Overholtzer, M.; Oyagi, A.; Pagnussat, G. C.; Park, J.; Ran, Q.; Rosenfeld, C. S.; Salnikow, K.; Tang, D.; Torti, F. M.; Torti, S. V.; Toyokuni, S.; Woerpel, K. A.; Zhang, D. D. Ferroptosis: A Regulated Cell Death Nexus Linking Metabolism, Redox Biology, and Disease. *Cell* **2017**, *171* (2), 273–285.

For Table of Contents Only